

Photonuclear and atomic cross sections of ^{27}Al between 3 and 38 MeV

N. K. Sherman, W. F. Davidson, and J. Ahrens*

Division of Physics, National Research Council of Canada, Ottawa, Ontario, Canada K1A 0R6

(Received 6 February 1987)

The total cross section for photon absorption of Al was measured for energies between 3 and 38 MeV with a γ -ray spectrometer consisting of a liquid deuterium target viewed by a photoneutron time-of-flight detector. Corrections to the observed total cross section for background electromagnetic processes in the absorber were computed by a Monte Carlo method. Between 5 and 8 MeV where the photonuclear cross section σ_N is negligible and the uncertainty in the measurements is small, values of the atomic cross section σ_Z calculated by others systematically exceed the measured values by 0.7%. In this energy interval σ_Z is mainly due to incoherent photon scattering by atomic electrons. Nonrelativistic atomic form factors and estimated radiative corrections used in calculating the tabulated incoherent scattering cross sections introduced enough uncertainty to justify decreasing σ_{incoh} by 0.87% to bring σ_Z into agreement with experiment. Correcting this discrepancy causes the integral between 10 and 38 MeV of σ_N , which has a maximum value of about 5% of σ_Z , to increase by 18% to 500 MeV mb. We conclude that the giant dipole resonance of ^{27}Al has a strength of 1.24 classical sum rule units.

INTRODUCTION

The integral over energy of the photonuclear cross section is the nuclear analog of the sum of the oscillator strengths for photon absorption by atomic electrons. In the atomic case the absorption strength is proportional to the atomic number Z . Dipole absorption associated with the relative motion of rigid, pointlike nucleons is proportional to NZ/A where N is the number of neutrons and A is the total number of neutrons and protons. It was recognized early on that the nuclear integrated cross section Σ is increased by absorption associated with mesonic degrees of freedom, nuclear spin flips, and higher multipoles. Recently there has been theoretical clarification concerning how much of the mesonic, or exchange, contribution is already included in the classical Thomas-Rieche-Kuhn sum rule adapted to the nucleus.

Two classes of experiment have yielded values of Σ . One class measures every photonuclear reaction cross section for a given nucleus, integrates each over all solid angles and energies, and sums over all the reaction channels. In practice results from different laboratories have to be combined, with consequent uncertainties of normalization. The other approach is to measure the total cross section for photon absorption at all energies, subtract the total non-nuclear cross section, and integrate over energy. This prevents omission of reaction channels and avoids angular integrations and relative normalizations. However, since the atomic absorption is much stronger than the photonuclear absorption, small absolute experimental or theoretical errors cause large percentage errors in Σ . Accuracy also requires thick, uniform, monoisotopic absorbers, and good absorption geometry. Fortunately there are cases where the atomic cross section σ_Z can be measured at energies where the photonuclear cross section σ_N is negligible, and can be

reliably extrapolated into the region where σ_N of a single isotope contributes. This is the case with ^{27}Al .

The total photonuclear cross section $\sigma_N(\omega)$ of an isotope of the element having atomic number Z can be obtained by measuring the total absorption cross section $\sigma(\omega)$ of the isotope for photons of energy ω and subtracting from it the atomic cross section $\sigma_Z(\omega)$ of the element. The maximum value of $\sigma_N(\omega)$ is about 30 times smaller than $\sigma_Z(\omega)$. The measurement must be done with care and $\sigma_Z(\omega)$ must be known precisely. At the present time σ_Z can be calculated with an uncertainty of about 0.2% for light elements. Tables of σ_Z are available¹ for $1 \leq Z \leq 100$ and $0.1 \text{ keV} \leq \omega \leq 100 \text{ GeV}$. For heavy elements the cross section values in the MeV energy range are known to be somewhat better than 1%. We have been engaged in a program at the National Research Council of Canada (NRC) to measure σ for isotopes over a wide range of Z to a precision of better than 0.5% for ω between 3 and 38 MeV by a method²⁻⁴ different from those previously used.

We employed a spectrometer consisting of a liquid deuterium target viewed by a photoneutron time-of-flight detector. The spectrometer can detect γ rays whose energies exceed a threshold value slightly greater than the 2.2246-MeV binding energy of ^2H . With energy resolution remaining less than 3% up to about 40 MeV, study can be carried out not only of the energy region of the giant dipole resonances where most photonuclear absorption occurs, but also below the particle threshold of most nuclei where the total photon cross section is essentially equal to σ_Z and can be compared with corresponding theoretical values of $\sigma_Z(\omega)$.

We chose Al as a small- Z , monoisotopic element suitable for accurate measurements of total absorption. It can be obtained in very pure form and is readily machined into a dimensionally stable absorber, which is

free of voids, and inert in air. The total absorption cross section of Al for photons has been measured previously,⁵⁻⁷ the best known results⁸ being for ω greater than 10 MeV. Some theoretical calculations have been made⁹ of the photonuclear cross section of ^{27}Al . Interest has been renewed in the integral of σ_N over photon energy because of theoretical progress on sum rules and exchange forces in nuclei¹⁰⁻¹⁴ and because of recent experiments^{2,15-17} which have attempted to resolve discrepancies between measured values of the integrated cross sections of nuclei.

Accurate experimental values of σ for ^{27}Al have been reported¹⁸ at 6.418 and 7.646 MeV. They were obtained by nuclear resonance techniques and ought to be free of systematic errors due to in-scattering and other electromagnetic backgrounds. Values of σ were found which are smaller than σ_Z calculated¹ by Hubbell, Gimm, and Øverbø by slightly more than the uncertainty in σ_Z estimated¹⁹ by Gimm and Hubbell. In two separate experiments^{2,4} we have measured $\sigma(\omega)$ for Al with precision, accuracy, and repeatability comparable to the theoretical uncertainty in σ_Z . In the second experiment the Al absorber was of the same dimensions as a single crystal Si absorber whose mass was measured²⁰ at the same time with the same apparatus. The Si density agreed to within one part in 10^5 with the accepted value for $\rho(\text{Si})$ which is uncertain by a few parts in 10^6 . We believe that uncertainty in $\rho(\text{Al})$ of the new absorber is about 1 part in 10^5 . The same value of $\rho(\text{Al})$, with an uncertainty of 0.3%, had been obtained for the old absorber. To obtain 0.1% uncertainty in σ we need only about 1 part in 10^4 uncertainty in the mass per unit area, which unlike ρ does not require measurement of the absorber length. The repeatability of the experiment indicates that this was certainly achieved in the first experiment also. We report here the combined results of both experiments, combined according to statistical weights, and corrected by about 0.2% to account for electromagnetic background effects not previously included. These corrections were computed^{21,22} using a Monte Carlo program²² written by Ahrens. The uncertainty in our experimental data between 4 and 12 MeV is comparable to that of the values of σ_Z calculated from theory in this energy region. A serious test of the tabulated values¹ is therefore possible in this case of small Z . We find the agreement very good between 5 and 8 MeV. We have corrected the incoherent contribution to σ_Z by 0.87% before using calculated values of σ_Z to extract photonuclear cross section values from our measurements of σ at higher energies.

EXPERIMENTAL

The experiment consisted of measurement of the ratio of photon flux F transmitted by an Al absorber to the flux F_0 incident on it. The relation

$$F(\omega) = F_0(\omega)e^{-n\sigma(\omega)} \quad (1)$$

gives the absolute value of $\sigma(\omega)$ when the number n of atoms per unit area of the absorber is known accurately. Photons were observed by detecting photoneutrons they

produced by the $^2\text{H}(\gamma, n)$ reaction in a liquid deuterium (LD_2) target behind the absorber. The energy of a photon was found by measuring the flight time of the photoneutron it ejected from the LD_2 target. The absorber was periodically inserted in a beam of pulsed bremsstrahlung produced in a radiator exposed to 42 MeV electrons from the NRC linac. The time-of-flight (TOF) resolution was 0.3 ns/m. The entire photon energy interval of $3 \leq \omega \leq 38$ MeV was covered in each measurement, with energy resolution of $0.36\% \leq \Delta\omega/\omega \leq 3.2\%$.

The LD_2/TOF spectrometer and the experimental techniques have been described before.^{2,3} One-quarter of the present data were reported in Ref. 2. The counting statistics were doubled²³ by Sherman. Using a new absorber, Sherman and Davidson repeated the experiment. They reported⁴ the new data combined with the first set of measurements. In the present work the data^{2,4} have been reanalyzed and additional small corrections have been applied to the complete ensemble of Al data.

Photoneutron flight time was measured by starting a time-to-digital converter (TDC) on the bremsstrahlung pulse and stopping it on the neutron recoil in the detector. The TDC was calibrated as described earlier² using sharp absorption resonances in the $^{12}\text{C}(n, n')$ reaction. At intervals, a graphite absorber was placed in the flight path between the LD_2 target and the neutron detector. Data from each calibration was fitted by least squares to the absorption resonances. The $\sigma(\omega)$ for Al of Sherman, Ross, and Lokan were weighted averages at each ω of σ from many measurements individually calibrated from ^{12}C resonances located to within 0.5 channel (2.2 ns) prior to the least squares fit.² In order to combine the new⁴ and old² Al data, all the calibration runs have been reanalyzed. Distinctive features in the ^{12}C cross section—six major resonances, and one sharp minimum at 3010 keV—were located with a precision of about ± 0.05 channel by fitting them to Gaussian shapes. The least squares fit was then repeated to verify the TDC slope. The $^{12}\text{C}(n, n')$ features extended over about 500 time channels of the 1024 channels available, and over a neutron energy range of 2 to 8 MeV. The calibrated region was enlarged to about 600 channels by introducing a large delay in the “stop” line carrying detector signals to the TDC. No significant deviation from linearity was detected.

The slope of the TDC calibration curve was found to be essentially constant from run to run and extremely linear (see Table II of Ref. 2).

The position of an absorption line varied by no more than one or two channels over periods exceeding six months. We assumed that the TDC slope was the same for all runs. From each calibration run the change in intercept was computed by which the corresponding absorption data set had to be shifted to line up with all the other data sets. The first and second halves of the data were treated as being from different experiments, since different absorbers were used. The corresponding data sets were added separately together and cross section values were obtained from them. The two sets of cross section values agreed within statistical uncertainty.

Between 5 and 8 MeV the first cross section data set

TABLE I. The parameters a_i, b_i, c_i of a second order polynomial fit [Eq. (1)] to the raw cross section data are listed for the results of Experiment 1 [Al data of Ref. 2 plus data taken by Sherman with the same absorber (see Ref. 4)] ($i=1$) and Experiment 2 [Data taken with new absorber by Sherman and Davidson (see Ref. 4)] ($i=2$).

i	a_i (mb)	b_i (mb/MeV)	c_i (mb/MeV ²)
1	1888±78	172.9±23.1	9.06±1.70
2	1777±78	136.2±23.1	6.18±1.70

($i=1$) and second set ($i=2$) can be fitted by second order polynomials:

$$\sigma_i(\omega) = a_i - b_i\omega + c_i\omega^2, \quad i = 1, 2. \quad (2)$$

Table I lists the values of the parameters for each case. When the second fitted curve is subtracted from the first, we obtain the average discrepancy

$$\Delta\sigma(\omega) = (112 \pm 110) - (36.6 \pm 32.6)\omega + (2.88 \pm 2.40)\omega^2 \text{ mb},$$

which shows that the functional forms of the two fits are very similar.

The two values at each ω were weighted according to statistics and combined to form a weighted average. The result⁴ was corrected for air displacement and geometrical in-scattering. New corrections calculated by a Monte Carlo method have now been applied to the observed cross section to compensate for in-scattering and other background effects. These will be described below.

It was noted that some uncertainty in ω arises from uncertainty in θ , the angle of neutron detection relative to the direction of the incident photons, which was estimated to be about $\pm 2^\circ$. Since then, θ has been measured carefully. We reexamine two effects here: (i) the spread in ω due to the finite solid angle subtended by the neutron detector at the LD₂ target, and (ii) the magnitude of uncorrected systematic error in our previous measurements due to a small departure of the angle of observation from 90° .

The photon energy can be expressed²⁴ in terms of the observed photoneutron kinetic energy T_n and its observed angle of emission θ :

$$\omega = \frac{T_n[1 + (m_n - B)/m_p] + B[1 - B/2m_p]}{1 - (T_n + B)/m_p + [T_n(T_n + 2m_n)]^{1/2} \cos\theta/m_p}, \quad (3)$$

where m_n, m_p are the rest mass energies of the neutron and proton and B is the neutron separation energy of the deuteron (2.2246 MeV).

For small T_n the denominator $D(T_n, \theta)$ is nearly independent of $\cos\theta$:

$$D(0) \simeq 1 - B/m_p. \quad (4)$$

The largest T_n in this experiment is about 20 MeV, for which

$$D(20, \theta) = 0.9763 + 0.2077 \cos\theta.$$

The neutron detector subtended a total angle of about 0.45° at the LD₂ target. The relative energy spread $\Delta\omega/\omega$ introduced by $\Delta\theta$ of $\pm 0.225^\circ$ is $\pm 0.096\%$ at 42 MeV decreasing to $\pm 0.066\%$ at 22 MeV (where $\Delta\omega$ is ± 14 keV). This is much smaller than the uncertainty in ω introduced by the time-of-flight resolution, and can be neglected.

The departure from 90° of the angle between the photon beam axis and the center of the neutron detector was measured²⁵ with a laser beam and an accurate prism. The detection angle was found to be 90.12° , so that $\cos\theta = -2.086 \times 10^{-3}$. The slight discrepancy from 90° requires that ω be increased by 0.04% at 42 MeV—that is, by 19 keV—from the value obtained when θ was assumed to be exactly 90° . For 10-MeV photons this systematic correction is +2 keV. This correction has also been neglected.

The values of ω listed in Table II have been corrected as in Ref. 2 for small systematic discrepancies between the neutron energies given by the least square fit to the calibration data and the accepted values.^{26,27}

The observed cross section is slightly smaller than the true value of $\sigma(\omega)$. This discrepancy arises from the experimental geometry, from regeneration of photons in the absorber, and from scattering of secondary photons and electrons (which may reradiate) into the detection solid angle. The discrepancy can be minimized by having a very small detection solid angle, a parallel beam of

TABLE II. Corrections $\delta(\omega)$ to the observed values of the total absorption cross section are listed for photon energies ω between 4 and 8 MeV where the photoneuclear cross section is negligible. The corrections δ_a for air displacement, δ_s for geometrical in-scattering, and δ_b for other background processes are shown as percentages of $\sigma_Z(\omega)$, the calculated atomic cross section (Ref. 1). The discrepancies $\epsilon_\sigma(\omega)$ between the corrected experimental values $\sigma(\omega)$ and $\sigma_Z(\omega)$ are also shown.

ω (MeV)	δ_a/σ_Z (%)	δ_s/σ_Z (%)	δ_b/σ_Z (%)	δ (mb)	σ (mb)	σ_Z (mb)	ϵ_σ (mb)
4	0.0465	0.120 ^a	0.200 ^b	+5.1	(1366±6 ^c)	1392±3	(-26)
5	0.046	0.125 ^a	0.190 ^b	+4.6	1264±14 ^d	1271±2.5	-7.4
6	0.0455	0.130 ^a	0.180 ^b	+4.2	1181±13 ^d	1190±2	-8.8
7	0.045	0.134 ^a	0.171 ^b	+4.0	1126±13 ^d	1133±2	-7.0
8	0.044	0.139 ^a	0.161 ^b	+3.8	1083±12 ^d	1092±2	-8.2

^aAverage for the two data sets calculated by the method of Ref. 2.

^b $\delta_b = \delta_{MC} - \delta_s$, where δ_{MC} is the background correction found by Monte Carlo calculations.

^cStatistical uncertainty in the observed value at 4.013 MeV.

^dUncertainty in value derived from a polynomial fit to the data between 5.5 and 8 MeV.

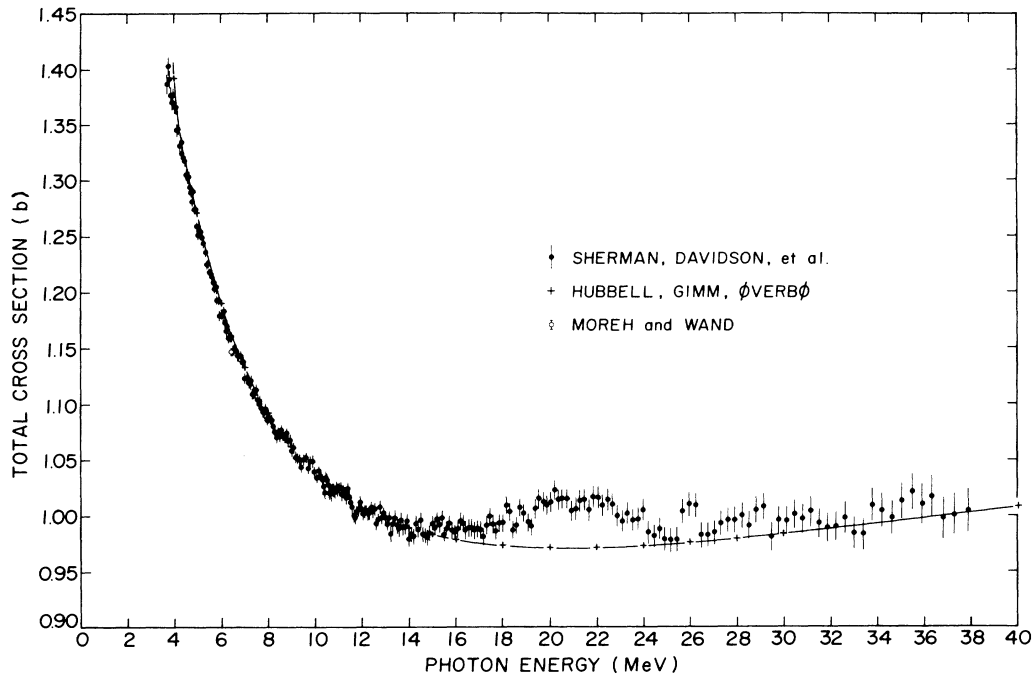


FIG. 1. The weighted averages of measurements of the total cross section of Al for absorption of photons are plotted (solid circles) vs photon energy. The error bars represent one standard deviation due to counting statistics. The crosses represent values of the atomic cross section listed in Ref. 1. The area bounded by the circles and the broken line is due to nuclear absorption.

incident photons, good collimation of the incident and transmitted beams, and diameters of the photon beam and absorber closely matched to the target diameter. In this experiment the LD₂ target subtended 1.06 msr at the radiator.

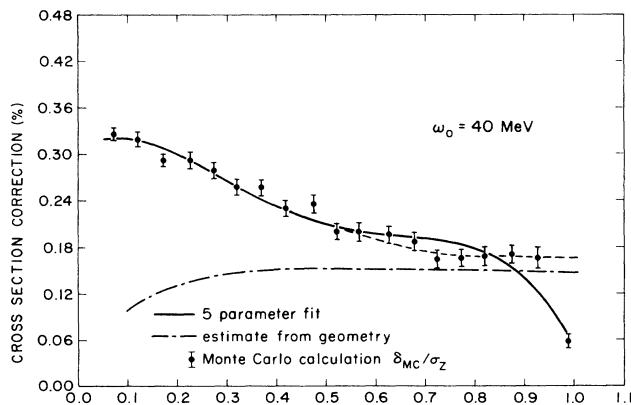


FIG. 2. The fraction δ_{MC}/σ_Z of the atomic cross section σ_Z by which the observed absorption cross section must be increased to correct for in-scattering and regeneration of photons is shown as a function of the fractional photon energy ω/ω_0 for a maximum photon energy ω_0 of 40 MeV. The correction δ_{MC} was calculated by a Monte Carlo method using an approximation to the actual experimental geometry. For $\omega/\omega_0 < 0.55$, the solid curve, a polynomial fit to the computed points was used. It has been extrapolated (dashed curve) beyond $\omega/\omega_0 \geq 0.7$ ignoring the highest energy point. The dashed-dotted curve represents the relative contribution δ_s/σ_Z due to geometrical in-scattering.

Although other experiments^{8,28} have had better geometry, the geometrical effects on the present results are still only fractions of a percent and have been corrected for. Good geometry allows most of the photons scattered forward after Compton interactions to avoid detection. The remaining “geometric in-scattering” is easily calculated^{2,29} and corrected for. The results for Al are shown in Fig. 1.

The Al absorber used in the first experiment was 178 mm long, and was 200 mm long in the second. In both cases the absorber was situated approximately midway between the radiator and the LD₂ target. The midplane of the target was 2.56 m from the radiator. In the first experiment the absorber was 53 mm in diameter—considerably larger than necessary to occult the 47-mm diameter LD₂ target. Photons initially directed outside the solid angle subtended by the target at the radiator could illuminate almost the entire cross section of the absorber at the end closest to the target. This penumbra was possible because of the finite size of the beam spot. A small fraction of the misdirected photons could be scattered by the Gray-Compton effect into the LD₂ thereby reducing the observed cross section by an amount δ_s . The solid angle subtended by the absorber at the target was used in calculating δ_s in this case. In the second experiment the Al absorber was 35 mm in diameter. It was held by four hollow Al cylinders 53 mm in diameter and 25 mm long, equally spaced. This approximately halved the thickness of Al traversed by misdirected photons. When calculating δ_s for the second experiment, we therefore assumed that the diameter of the LD₂ target established the in-scattering solid angle. The

values of δ_s in Table II are an average of the two, very similar, sets of values.

To correct for rescattering and regeneration of photons is not straightforward.^{17,30,31} Phenomena to be considered include radiation by the electron or positron of a pair created by absorption of an incident photon, annihilation in flight of the positron of a pair, radiation by a photoelectron or Compton electron produced in the absorber, rescattering into the detection solid angle of a photon scattered out of it, etc. Monte Carlo techniques can be used to simulate production of secondary photons in a specified experimental arrangement.

A hybrid computing routine has been written²² which combines Monte Carlo features with analytical approximations of physical processes such as multiple scattering of electrons and energy partitions between the electron and positron in pair creation. This program assumes that the photon beam, the collimator apertures, the absorber, the target, and the radiator are square in cross section, whereas the present experiment exhibited cylindrical symmetry about the beam axis. Using this program we have calculated the corrections for background processes assuming square shapes of the same areas as the actual circular shapes. The corrections are small, so this departure from reality should be of little consequence.

Figure 2 shows the percentage discrepancy $\delta_{\text{MC}}/\sigma_Z$ to be expected between the observed atomic cross section and its true value, calculated for the experimental geometry by the hybrid Monte Carlo technique. The calculations were performed for a maximum photon energy ω_0 of 40 MeV rather than (41.4 ± 1.6) MeV corresponding to the maximum electron energy E_0 of about 42 MeV actually used. The effect of this difference is negligible. Over the fractional energy range $0.05 \leq \omega/\omega_0 \leq 0.55$ the solid curve, a five-parameter fit to the calculated discrepancies $\delta_{\text{MC}}/\sigma_Z$, was used. For $\omega/\omega_0 \geq 0.8$ the fitted curve departs from physical reality because of the effect of the highest energy value of δ_{MC} which is too small because of a computational detail associated with the vanishing of the bremsstrahlung spectrum at $\omega/\omega_0 = 1$. The geometrical, Compton in-

scattering does not vanish at high energy—rather, δ_s is constant. Since σ_Z for Al is nearly constant between 20 and 40 MeV, δ_s/σ_Z is also approximately constant. It decreases for $\omega/\omega_0 \leq 0.4$ because σ_Z increases rapidly as ω decreases. This contribution to the reduction of the observed cross section is indicated by the dashed-dotted curve. We have neglected the highest energy computed point and have extrapolated (dashed curves) the total relative discrepancy $\delta_{\text{MC}}/\sigma_Z$ through the five other computed points having $\omega/\omega_0 \geq 0.7$ so as to be parallel to the trend of δ_s/σ_Z . The dashed and solid curves have been joined smoothly over the interval $0.55 \leq \omega/\omega_0 \leq 0.75$. One sees that at 36 MeV the simple geometrical prescription² for δ_s/σ_Z accounts for 89% of the apparent reduction—by 0.17%—of the observed cross section by all background processes. For energies less than 25 MeV, however, other processes are significant. At 10 MeV they contribute equally to the total reduction which is 0.29%. At the lowest energies the other processes dominate in the apparent reduction of σ_Z by about 0.32%.

Table III compares the geometrical corrections δ_s/δ_Z previously applied to the observed cross section values, with the complete corrections $\delta_{\text{MC}}/\sigma_Z$ calculated by the hybrid Monte Carlo method. The amounts $\Delta\sigma(\omega)$ by which the Al cross sections reported earlier need to be increased are also listed. Between 13 and 38 MeV the effect of these corrections is to increase the integrated cross section by

$$\sum_i (\Delta\sigma)_i \hat{\omega} = 10.3 \text{ MeV mb} .$$

where $i = 13$ to 38 labels the correction for each 1-MeV interval $\hat{\omega}$.

The air displacement correction, originally⁴ taken to be constant and equal to 0.5 mb, in fact decreases slowly with increasing energy from 0.38 mb at 13 MeV to 0.32 mb at 38 MeV (independent of absorber length). The integrated cross section has been reduced by 3.8 MeV mb to correct for this.

The measured photonuclear cross section integrated from 13 to 38 MeV is, through these improvements, in-

TABLE III. Variation with photon energy ω of the additional corrections $\Delta\sigma$ to be made to the values of the total cross section of Al reported in Ref. 4 which were corrected by + 1.49 mb for δ_s , the apparent reduction caused by geometric in-scattering, and by + 0.5 mb for δ_a , the air displacement effect. The apparent reduction δ_{MC} due to in-scattering, calculated by a Monte Carlo method, is shown as a percentage of the atomic cross section σ_Z .

ω (MeV)	σ_Z (b)	δ_s/σ_Z (%)	$\delta_{\text{MC}}/\sigma_Z$ (%)	$\Delta\sigma$ (mb)
4	1392	0.107 ^a	0.320	+2.96
8	1092	0.136 ^a	0.300	1.79
12	1008	0.148	0.265	1.18
16	978.8	0.152	0.233	0.79
20	971.4	0.153	0.210	0.55
24	973.3	0.153	0.190	0.36
28	979.7	0.152	0.175	0.22
32	988.6	0.151	0.168	0.17
36	998.3	0.150	0.167	0.17
40	1008	0.148	0.166	+0.18

^aThe average values of δ_s in Table II are slightly different.

creased by about 2% over the value reported previously.⁴ Note that Ref. 4 contains a misprint: Although the reported value of $1.00\Sigma_{\text{TRK}}$ was correct for the integrated cross section expressed in terms of the nuclear Thomas-Rieche-Kuhn sum rule, the equivalent in MeV mb should have been (404 ± 66) . This value becomes (410 ± 56) MeV mb when the additional corrections are applied. In sum rule units this is $(1.02\pm 0.14)\times\Sigma_{\text{TRK}}$, where

$$\Sigma_{\text{TRK}} = (2\pi^2 e^2 \hbar / Mc)(NZ/A), \quad (5)$$

and e is the charge of the proton, \hbar is Planck's constant divided by 2π , M is the mass of a nucleon, N is the neutron number of the absorbing nucleus, and A is the number of nucleons. We have used the value 59.74 MeV mb for the constant factor multiplying NZ/A .

The above is still not our final value, however. Table II shows a small systematic discrepancy of about 8 mb between the tabulated values of σ_Z and our corrected measurements, which are smaller. We have modified σ_Z , as described in the next section, to remove the discrepancy before extracting the total photonuclear cross section.

RESULTS

The measured total cross section for photon absorption by Al is shown in Fig. 1 for energies between 3 and 38 MeV. The solid circles are weighted average values of $\sigma(\omega)$. The error bars indicate the standard deviations of the points due to counting statistics. The crosses are values of the atomic cross section tabulated¹ by Hubbell, Gimm, and Øverbø. The area between the broken line and the data points is due to absorption by the Al nucleus.

Figure 3 shows the low energy region in more detail. Weighted average values of the measured $\sigma(\omega)$, shown as solid circles, have been corrected for air displacement, in-scattering, and photon regeneration. The solid curve is a least squares fit by a second order polynomial to the data points. Over the interval $5 \text{ MeV} \leq \omega \leq 8 \text{ MeV}$ the calculated values of $\sigma_Z(\omega)$ from Ref. 1 are well fitted by the third order polynomial

$$\begin{aligned} \sigma_Z(\omega) = & (2354 \pm 41) - (364.6 \pm 19.3)\omega \\ & + (36.08 \pm 2.87)\omega^2 - (1.28 \pm 0.14)\omega^3 \text{ mb} . \end{aligned}$$

This is plotted as the dashed curve in Figure 3. The experimental data between 5.5 and 8 MeV are well fitted by a second order polynomial, allowing the measured total cross section to be written as

$$\begin{aligned} \sigma(\omega) = & (1822 \pm 56) - (151.6 \pm 16.5)\omega \\ & + (7.41 \pm 1.21)\omega^2 + \delta(\omega) \text{ mb} , \end{aligned}$$

where $\delta(\omega)$ corrects for air displacement, in-scattering, and photon regeneration.

A good second order fit to $\sigma_Z(\omega)$ can also be obtained, which has similar parameters to the expansion of $\sigma(\omega)$:

$$\sigma_Z(\omega) = 1978 - 185.8\omega + 9.25\omega^2 \text{ mb} .$$

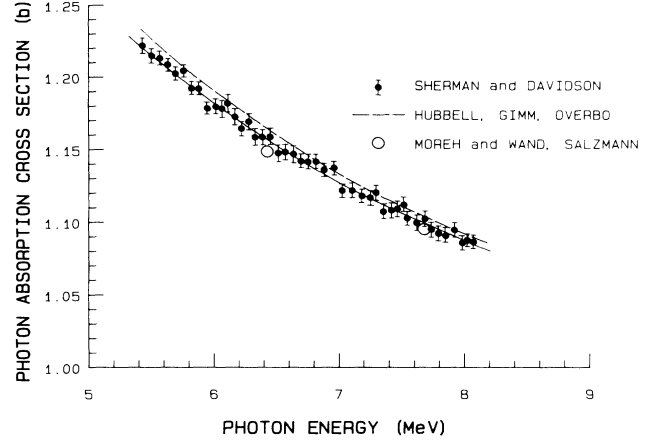


FIG. 3. For low energies, weighted average values of the measured Al total cross section (solid circles) are compared with atomic cross section values from Ref. 1. The open circles are the result of resonance fluorescence measurements (Ref. 18). The solid curve is a least squares fit by a second order polynomial to the data points, subsequently corrected for air displacement, in-scattering, and photon regeneration. The broken line is a third order fit to the tabulated values of $\sigma_Z(\omega)$.

The discrepancy at low energies between $\sigma(\omega)$ and $\sigma_Z(\omega)$ can therefore be written

$$\epsilon_o(\omega) = 156.3 - 34.15\omega^2 - \delta_{\text{MC}}(\omega) \text{ mb} ,$$

where the slowly varying air displacement correction δ_a of about 0.5 mb has been incorporated into the constant term and δ_{MC} is the remaining correction approximated²² by Monte Carlo methods. Some values of $\epsilon_o(\omega)$ are listed in Table II. The calculated values of $\sigma_Z(\omega)$ lie on the average about 8 mb above the experimental values of $\sigma(\omega)$ for ω between 5 and 8 MeV.

When the photon energy is less than the lowest particle separation energy, which for ²⁷Al is the photoproton threshold at 8.2709 MeV, the only decay channel available for nuclear de-excitation is γ ray decay. The intrinsic widths of γ ray lines are very small and will be Doppler broadened to only a few electron volts, whereas the LD₂/TOF spectrometer resolution is tens of keV in this energy region. Observation of discrete transitions is thus not likely. The average cross section for photoabsorption by the nucleus is also expected to be very small. To a good approximation we expect that the measurements of $\sigma(\omega)$ up to 8 MeV are measurements of $\sigma_Z(\omega)$. Any finite nuclear contribution would in fact increase the discrepancy mentioned above.

Between 5 and 8 MeV, therefore, we find that the values of $\sigma_Z(\omega)$ tabulated in Ref. 1 are systematically 0.7% larger than our measured values. Does the method of calculation of σ_Z leave room for a discrepancy as large as 1%? We recall that at a given energy in the range of interest

$$\sigma_Z = \sigma_R + \sigma_{\text{GC}} + \sigma_{\text{pe}} + \sigma_t + \sigma_K , \quad (6)$$

where the subscripts denote Rayleigh (coherent) scatter-

TABLE IV. Summary of uncertainties in the measured total absorption cross section σ , integrated photonuclear cross section Σ , and photon energy ω introduced by properties of the absorber, experimental factors, and corrections. See Refs. 2, 3, 17, and 32 for further details.

Quantity	Value	Quality	Uncertainty in σ	Uncertainty in Σ	Uncertainty in ω
Atomic no.	13				
Isotope	27	100%			
Atomic weight	26.9815				
Length	178 mm				
	200 mm				
Diameter	53 mm				
	35 mm				
Mass/area	47.86	$\pm 0.10 \text{ g/cm}^2$	$\pm 0.14\%$	$\pm 4\%$	
	53.78	$\pm 0.11 \text{ g/cm}^2$			
Density	2.680	$\pm 0.006 \text{ g/cm}^2$			
Content					
Al	99.995%				
Mg	12 ppm				
Si	10 ppm				
Fe	10 ppm				
Cu	30 ppm				
In-scattering	0.13%				
Counting loss at 8 MeV	5%		$\pm 0.2\%$	$\pm 5\%$	
Air displacement	0.045%				
Photon regeneration					
at 4 MeV	0.16%		$\pm 0.03\%$	$\pm 1\%$	
at 40 MeV	0.01%				
Reproducibility					
at 5 MeV	$\pm 0.1\%$				
at 8 MeV	$\pm 0.3\%$		$\pm 0.2\%$	$\pm 5\%$	
Normalization of σ_{GC}	0.87%		$\pm 0.4\%$	$\pm 9\%$	
Statistics			$\pm 0.7\%$	$\pm 5\%$	
Timing resolution	0.23 ns/m				$0.4\% \leq \Delta\omega/\omega \leq 3\%$
Detector solid angle	48 μsr				$\pm 0.1\%$
Detection angle	90.12°				0.04%
Raw time calibration	± 0.5 channel				
Fitted data calibration	± 0.05 channel				
Drift	± 0.25 channel/ month				
TDC linearity before correction	$\pm 30 \text{ keV}$				$\pm 0.02\%$ at 10 MeV

ing, Gray-Compton (incoherent) scattering, photoelectric effect, triplet (pair creation on an atomic electron), and pair creation on the nucleus, respectively. Between 5 and 8 MeV σ_R and σ_{pe} are completely negligible, while σ_{GC} accounts for about 80% of σ_Z . Both σ_I and σ_K are believed to be uncertain by less than 1%. The former rises from about 4 mb to only 11 mb over the energy interval, and can therefore be ruled out as a source of the discrepancy. Similarly, it would require 3% or 4%

errors in σ_K to alter σ_Z by 1%. Such large errors appear unlikely since at 5 MeV the Coulomb correction is exact and proper relativistic form factors were used in the calculations. On the other hand, an error of only 0.87% in σ_{GC} suffices to explain the discrepancy. Indeed, a nonrelativistic Hartree-Fock incoherent scattering function was used by Hubbell *et al.* Furthermore the radiative correction was extrapolated in an *ad hoc* fashion. We therefore assume that σ_{GC} is overes-

timated, and everywhere by the same percentage.

Between 15 and 30 MeV the atomic cross section of Al is constant to within $\pm 1\%$. The fraction σ_{GC}/σ_Z declines from 55% at 13 MeV, to 35% at 24 MeV, to 28% at 38 MeV. It is straightforward to correct the integrated photonuclear cross section for the overestimate in σ_Z . The correction is considerable, namely, 90 MeV-mb, which increases Σ by 18%. It also lowers the energy at which σ_N is seen to begin to contribute, from 13 MeV observed from the raw data, down to about 10 MeV. We estimate that the uncertainty in the correction to the integral can be as much as 50%, so the final result is

$$\int_{10}^{38 \text{ MeV}} \sigma(\omega) d\omega = (500 \pm 65) \text{ MeV mb},$$

when the uncertainties summarized in Table IV are added in quadrature.

CONCLUSIONS

Our result for the integrated photonuclear cross section of ^{27}Al up to 38 MeV is $(1.24 \pm 0.16)\Sigma_{\text{TRK}}$. The Mainz group⁸ found 739 MeV mb ($\pm 2.6\%$) for the integral of σ_N up to 100 MeV. In units of the classical sum Σ_{TRK} this is 1.83 ± 0.05 . Their Fig. 11 gives a value of 1.15 for the integral up to 35 MeV. From the inset to their Fig. 6 we estimate 1.18 ± 0.04 for Σ up to 38 MeV.

The 5% discrepancy between the Ottawa and Mainz values of $\Sigma(\text{Al})$ is consistent with the uncertainties in the two measurements. The small uncertainty in σ_Z quoted by the Mainz group, namely, 0.1%, may seem inconsistent with the 1% uncertainty suggested even by the authors of more recent, improved tables of atomic cross sections.¹ However, the Mainz group adjusted the old

values of σ_Z for light elements partly on the basis of comparisons with their measurements of absorption by heavy elements. The good agreement between the two experiments occurs when the present data are extracted using a slightly renormalized incoherent scattering cross section for Al.

We conclude that the evidence is firm for 20% more photon absorption in the giant dipole resonance of ^{27}Al than predicted by the classical dipole sum rule. Electric quadrupole, magnetic dipole, and mesonic absorption¹⁰⁻¹⁵ can account for it.

ACKNOWLEDGMENTS

We acknowledge with thanks the excellent technical support and reliable linac operation provided by A. Nowak, M. Kosaki, and D. Kleinbub. The computer system for taking and reducing data was maintained by C. K. Ross. The absorber masses were determined by D. G. Kearney, R. Butland, and P. G. R. Gendron. Word processing was carried out by C. M. Kingston, H. Matchett, and J. Perratt. The figures were drawn by R. Matsumura and A. Thompson. The Al for the absorbers was donated by Alcan Limited. The absorbers were machined by F. H. Schuh and H. J. Dickson in the Mechanical Components Laboratory of the Division of Physics. One of us (N.K.S.) enjoyed the hospitality of B. Ziegler and J. Ahrens during a brief stay at the Max-Planck-Institut für Chemie, Mainz, and of the Laser and Plasma Physics Section at NRC where this work was completed. Discussions with H. Gimm about atomic cross sections were useful. The interest of J. H. Hubbell in this work and encouragement by R. Bergere are appreciated.

*Present address: Max-Planck-Institut für Chemie (Otto-Hahn-Institut), Mainz, Federal Republic of Germany.

¹J. H. Hubbell, H. A. Gimm, and I. Øverbø, *J. Phys. Chem. Ref. Data* **9**, 1023 (1980).

²N. K. Sherman, C. K. Ross, and K. H. Lokan, *Phys. Rev. C* **21**, 2328 (1980).

³N. K. Sherman and G. M. Ewart, *Phys. Rev. C* **27**, 1011 (1983).

⁴N. K. Sherman and W. F. Davidson, in *Proceedings of the Fourth International Symposium on Neutron-Capture Gamma-Ray Spectroscopy and Related Topics, Grenoble, 1981*, Vol. 62 of *Institute of Physics Conference Series*, edited by T. Von Egidy, F. Gonnenswein, and B. Maier (Institute of Physics, London, 1982), p. 630.

⁵J. M. Wyckoff, B. Ziegler, H. W. Koch, and R. Uhlig, *Phys. Rev.* **137**, B576 (1965).

⁶B. S. Dolbilkina, V. A. Zapevalov, V. I. Korin, L. E. Lazareva, and F. A. Nikolaev, *Izv. Akad. Nauk SSSR, Ser. Fiz.* **30**, 349 (1966).

⁷N. Bezic, D. Brajnik, D. Kamnick, and G. Kernel, *Nucl. Phys. A* **128**, 426 (1969).

⁸J. Ahrens, H. Borchert, K. H. Czock, H. B. Eppler, H. Gimm, H. Gundrum, M. Kroning, P. Riehn, G. Sita Ram, A. Zieger, and B. Ziegler, *Nucl. Phys.* **A251**, 479 (1975).

⁹L. N. Bolen and J. M. Eisenberg, *Phys. Lett.* **9**, 52 (1964); W.

H. Bassichis and F. Scheck, *Phys. Rev.* **145**, 771 (1966); D. V. Webb, E. G. Muirhead, and B. M. Spicer, *Nucl. Phys.* **A159**, 81 (1970).

¹⁰G. E. Brown and M. Rho, *Nucl. Phys.* **A338**, 269 (1980).

¹¹H. Arenhövel, *Z. Phys.* **A302**, 25 (1981).

¹²G. Goulard and B. Lorazo, *Can. J. Phys.* **60**, 162 (1982).

¹³A. Arima, G. E. Brown, H. Hyuga, and M. Ichimura, *Nucl. Phys.* **A205**, 27 (1973).

¹⁴H. Miazawa, *Prog. Theor. Phys. (Kyoto)* **6**, 801 (1951).

¹⁵P. Carlos, H. Beil, R. Bergere, B. L. Berman, A. Leprêtre, and A. Veyssiere, *Nucl. Phys.* **A378**, 317 (1982).

¹⁶B. L. Berman, R. Bergere, and P. Carlos, *Phys. Rev. C* **26**, 304 (1982).

¹⁷N. K. Sherman, W. F. Davidson, and A. Claude, *J. Phys. G* **9**, 1519 (1983).

¹⁸R. Moreh and Y. Wand, *Nucl. Phys.* **A252**, 423 (1975); R. Moreh, D. Salzmann, and Y. Wand, *Phys. Rev.* **30B**, 536 (1969).

¹⁹H. A. Gimm and J. H. Hubbell, National Bureau of Standards Technical Note 968 (U.S. GPO, Washington, D.C., 1978), p. 13.

²⁰G. D. Chapman, R. Butland, and D. G. Kearney (private communication).

²¹N. K. Sherman and J. Ahrens (unpublished).

²²J. Ahrens, MPI (Mainz) program TOGA (1981); revised ver-

- sion TOGA (1983).
- ²³N. K. Sherman, 1979: Measurements with absorber of Ref. 1, included in data set of Ref. 3.
- ²⁴N. K. Sherman, Nucl. Instrum. Methods **79**, 197 (1970).
- ²⁵A. Nowak, M. Kosaki, and N. K. Sherman (unpublished).
- ²⁶S. F. Mughabghab and D. I. Garber, Brookhaven National Laboratory Report No. 325, 3rd ed. (U.S. Department of Commerce, Springfield, Virginia, 1973), p. 6-1.
- ²⁷R. B. Schwartz, R. A. Schrack, and H. T. Heaton, National Bureau of Standards Monograph 138 (U.S. Dept. of Commerce, Washington, D.C., 1974), pp. 26 and 27.
- ²⁸G. M. Gurevich, L. E. Lazareva, V. M. Mazur, G. V. Solodukhov, and B. A. Tulupov, Nucl. Phys. **A273**, 326 (1976).
- ²⁹L. C. Henry and T. J. Kennett, Can. J. Phys. **49**, 1167 (1971).
- ³⁰N. K. Sherman, W. F. Davidson, A. Novak, M. Kosaki, and J. Roy, Phys. Rev. Lett. **54**, 1649 (1985).
- ³¹N. K. Sherman, W. F. Davidson, S. Raman, W. Delbianco, and G. Kajrys, *Capture Gamma-Ray Spectroscopy and Related Topics, Knoxville, Tennessee, 1984*, AIP Conference Proc. No. **125**, edited by S. Raman (AIP, New York, 1985), p. 221.
- ³²N. K. Sherman and G. M. Ewart, Can. J. Phys. **59**, 914 (1981).